Journal of Engineering, Emerging Technologies and Applied Sciences

Volume: 03 Issue: 01 | March, 2026 Access point: **https://www.ndu.edu.ng/jeetas**

Optimal Placement of Harmonic Filters in Electric Power Networks: Eko Distribution Network as Case Study

* Felix O. Kalunta [1], Francis N. Okafor[2], Sunday Adetona[3], Adeola Balogun[4], Osita Omeje[5]

[1] *Department of Electrical & Electronics Engineering, Abia State University, Uturu*

[2,3,4,5] *Department of Electrical & Electronics Engineering, University of Lagos, Akoka, Lagos*

**Email: felikap@gmail.com*

ABSTRACT

Many researchers have proposed the attenuation of injected harmonic magnitudes with electronic filters as the panacea for resonance problems in electric power distribution networks. Identifying suitable ratings and locations for the filters is a subject of on-going research, and Genetic Algorithm has been deployed on certain occasions as meta-heuristic optimization method for the optimal location of such compensation devices. This paper has proposed a guide based on a non-linear loop current analysis in time domain, with the total harmonic distortion and current amplification at several parts of the network employed as parameters for filter location because they portray the danger or risk level imposed on each section of the network by resonance. The creation of dummy loops is also introduced to accommodate the connection of capacitor banks, filter branches and cable capacitances during the network calculations. The developed tool has successfully been applied to a section of Eko distribution network in Lagos Metropolis which contains induction furnaces at two load centers. A passive filter was designed and applied in two locations where the highest current amplifications were attained. Verification of the designed filter has revealed a significant decrease in the magnitude of 5th order harmonic current and outright elimination of 107th order harmonic current. The proposed technique will guide the Power Quality Engineer in identifying the resonance conditions at the design or modification stage of electric power networks as well as undertaking adequate precautionary measures to minimize resonance events and the associated economic losses.

Keywords — Amplification Factor; Dummy Loop; Distortion Profile; Filter; Resonance.

1. INTRODUCTION

Power Quality Issues refer to problems in the electric power supply that cause deviation from the normal values of voltage, current, or frequency and adversely affect the performance of electrical equipment. Common power quality issues are voltage dip, voltage swell, phase unbalance, voltage flicker while their common causes are non-linear loads (computers, UPS, drives for instance), starting of large motors, system faults, switching operations, lightning and weather conditions etc. Among other power quality issues facing system operators, harmonic distortion caused by the presence of non-linear loads is a major source of concern because of its inherent hazardous effects on power transformers, switchgear, power cables, neutral conductors etc. (Manikandan *et. al.*, 2013). The most common sources of harmonic distortion include rectifiers, induction furnaces, arc producing devices (Bester and Atkinson, 2012). By Fourier theory, the distortion of electrical current is analogous to the injection of high order harmonics into the network, implying that the elimination of high order harmonics from the power network will contribute effectively to system stability and reliability. Several techniques including the use of mitigation filters have been devised as the means of mitigating the effect of harmonic distortion on power networks (Liberado *et. al.,* 2013). According to Kalunta *et. al.* (2016), filters can be installed by electricity consumers to prevent the internally generated harmonic currents from being propagated into the supply network. Typical designs of passive filters can be found in literature (Pejovic and Kolar, 2008; Kazeem *et. al.,* 2005).

Studies have also shown that harmonic pollution is a contributor to network resonance (Md Hasan *et. al.,* 2012) by amplifying the network currents to cause equipment breakdown or unexpected tripping of protective devices (Acha and Madrigal, 2001). The use of harmonic filters to dampen the critical harmonic magnitudes has proved to be an effective technique for resonance mitigation (Abdel Aleemet *et. al*., 2012). However, the optimal location of the harmonic filter in the power network which can guarantee effective mitigation is a subject of on-going research (Mohammed *et. al*., 2014). The use of distortion profiles obtained from time domain computation of network currents is proposed in this paper and illustrated using a section of Eko distribution network in Lagos as case study. Parameters like voltage profile, Distortion indices and amplification level of network currents at different locations provide sufficient insight in identifying the regions that are prone to resonance event in the power network. These were utilized in identifying the appropriate locations of filters in the system under study. The pivotal function model of rectifier based non-linear loads described in Kalunta and Okafor (2015) and use of dummy loops to represent the inclusion of cable shunt capacitance have been adapted to time domain analysis of power networks for more accurate determination of the actual distortion profile of network currents.

The Investigated Network

The single line diagram in Figure 1 represents a $33kV$ radial network extracted from the EKO distribution system in Lagos Metropolis. There are two load centers with induction furnaces at the installation stage namely the Unilag Engineering faculty and Foundry unit of Federal Institute of Industrial Research Oshodi (FIIRO) Lagos. The possibility of including an AC arc furnace in future at the Nigeria Railway Corporation (NRC) substation is also considered. The numbering of meshes 1 – 10 considered in the process corresponds to those of the feeders in the installation. The parameters of overhead lines, underground cables and load centers were computed in line with existing analytical procedures for power systems.

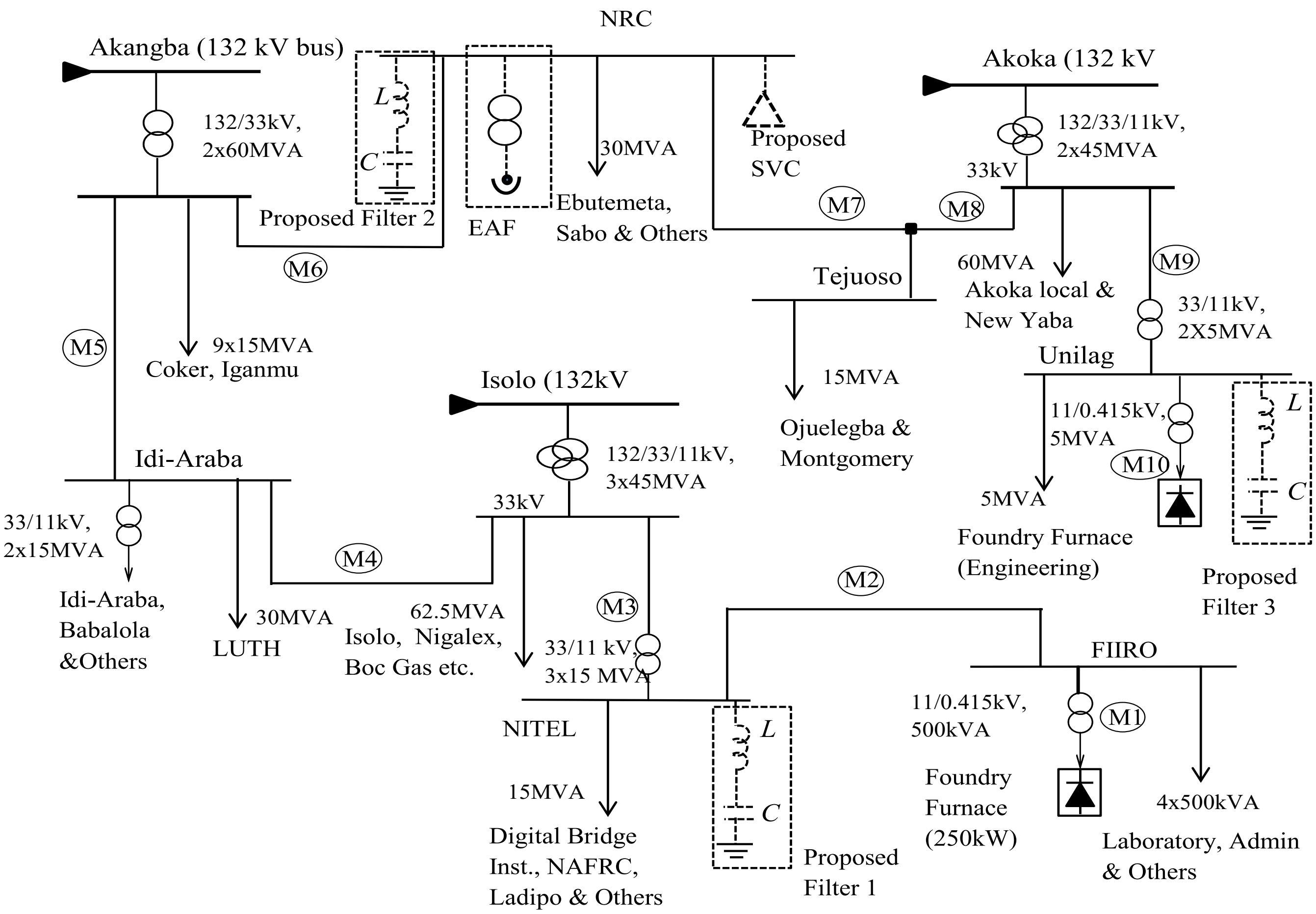

Figure 1: One-line diagram of the investigated 33 kV distribution network belonging to EKO Distribution Company Lagos

3. METHODOLOGY

The time domain computation of network currents is performed in this paper to determine the level of current amplification at different sections of the network and the associated total harmonic distortion (THD). The amplification factor as well as total harmonic distortion at any section of the network indicates the level of risk imposed at that point by resonance, and therefore provides a guide on the suitable locations of harmonic filters. Priority is then accorded to those sections with high current amplification in the placement of harmonic filters. The circuit analysis was implemented using matlab programing tools in accordance with the following algorithm;

i. Modelling of network components
ii. Computation of network matrices
iii. Network mesh analysis
iv. Determination of distortion profile

Network Modelling

An equivalent circuit of the network is drawn showing the loop currents, the 132 kV transmission supply in their Thevenin's equivalent, and each non-linear load represented as voltage vector in series with their respective load resistances. The induction furnace is represented by the pivotal function model equations of three-phase controlled rectifier at 45° firing angle as described in Kalunta *et al.* (2016). The phase 'a' model equation in a balanced three-phase controlled rectifier by pivotal function technique is,

$$i_a = \begin{cases} 0 & \forall \quad 0 < \omega t \le \frac{\pi}{6} + \phi + \alpha \\ \frac{\omega}{L_s}\sqrt{2}V_L \cos(\omega t) - \frac{1}{L_s P}\frac{di_a}{dt} & \forall \quad \frac{\pi}{6} + \phi + \alpha < \omega t \le \frac{2\pi}{3} + \alpha \\ -\frac{\omega}{L_s}\sqrt{2}V_L \cos(\omega t + \frac{2\pi}{3}) - \frac{1}{L_s P}\frac{di_a}{dt} & \forall \quad \alpha + \frac{2\pi}{3} < \omega t \le \frac{5\pi}{6} + \phi \\ 0 & \forall \quad \phi + \frac{5\pi}{6} < \omega t \le \pi \\ -i_a(\omega t - \pi) & \forall \quad \pi < \omega t > 2\pi \end{cases} \quad (1)$$

where $i_a > 0 \; \forall \; \omega t \le \pi$, and the current also obeys the half-wave symmetry, $i_a = -i_a(\omega t - \pi) \; \forall \; \pi < \omega t \le 2\pi$

$$P = \frac{\beta i_a}{4 + \beta i_a (2R_f + R_L)} \quad (2)$$

Where

α – thyristor firing angle, β = 38.7, R_L – Load Resistance, R_f – forward Resistance of thyristor, v_{ab} and v_{ac} represent instantaneous input voltages. The electric arc furnace model adopted in this study is the exponential-hyperbolic model (Hooshman *et al.*, 2008) which adequately represents the arc voltage v_{arc} of the EAF in the time domain as shown below.

$$v_{arc} = \begin{cases} V_{at} + \frac{C}{D + i_{arc}} & \frac{di_{arc}}{dt} \ge 0 \quad i_{arc} > 0 \\ V_{at}(1 - e^{-i_{arc}/I_0}) & \frac{di_{arc}}{dt} < 0 \quad i_{arc} > 0 \end{cases} \quad (3)$$

Where i_{arc} are the arc voltage and current of the EAF respectively, V_{at} is the threshold magnitude to which voltage approaches as current increases (which depends on the arc length) and I_0 is the current time constant in kA. The constants D and C are corresponding to the arc power and current respectively, and their values vary for increasing and decreasing states of the arc current. Thus, the electric arc length is configured to simulate three stages of loading, melting and the end of the process which is the refining stage. The lengths are different in each phase of the system thereby producing an unbalanced loading.

Computation of Network matrices

The network matrices for resistances R_{old}, inductances L_{old} and inverse capacitances G_{old} are first determined with the exclusion of cable capacitance. The expanded form of the network matrices are in these forms:

$$L_{old} = \begin{bmatrix} (L_1 + L_{s1}) & -L_{s1} & 0 & 0 & & \cdots \\ -L_{s1} & (L_{s1} + L_2 + L_{s2}) & -L_{s2} & 0 & & \cdots \\ 0 & -L_{s2} & (L_{s2} + L_2 + L_{s3}) & -L_{s3} & 0 & \\ 0 & 0 & -L_{s3} & \ddots & \vdots & \\ \vdots & \vdots & 0 & \vdots & (L_{s,n-1} + L_n + L_{sn}) & \end{bmatrix} \quad (4)$$

$$R_{old} = \begin{bmatrix} (R_1 + R_{s1}) & -R_{s1} & 0 & 0 & & \cdots \\ -R_{s1} & (R_{s1} + R_2 + R_{s2}) & -R_{s2} & 0 & & \cdots \\ 0 & -R_{s2} & (R_{s2} + R_2 + R_{s3}) & -R_{s3} & 0 & \\ 0 & 0 & -R_{s3} & \ddots & \vdots & \\ \vdots & \vdots & 0 & \vdots & (R_{s,n-1} + R_n + R_{sn}) & \end{bmatrix} \quad (5)$$

$$G_{old} = \begin{bmatrix} \frac{1}{C_{B1}} & -\frac{1}{C_{B1}} & 0 & \cdots \\ -\frac{1}{C_{B1}} & \left(\frac{1}{C_{B1}}+\frac{1}{C_{B2}}\right) & -\frac{1}{C_{B2}} & \cdots \\ 0 & -\frac{1}{C_{B2}} & \left(\frac{1}{C_{B1}}+\frac{1}{C_{B2}}+\frac{1}{C_{B3}}\right) & \cdots \\ \vdots & \vdots & \vdots & \ddots \end{bmatrix} \quad (6)$$

Where $\boldsymbol{L}_{old} - n \times n$ loop inductance matrix

$\boldsymbol{R}_{old} - n \times n$ loop resistance matrix

$\boldsymbol{G}_{old} - n \times n$ loop inverse capacitance matrix

$R_1, R_2, R_3, \ldots$ are the series resistances of power lines and cables

$L_1, L_2, L_3, \ldots$ are the series inductances of power lines and cables

$R_{s1}, R_{s2}, R_{s3}, \ldots$ are the shunt resistances at load centers

$L_{s1}, L_{s2}, L_{s3}, \ldots$ are the shunt inductances of at load centers

$C_{B1}, C_{B2}, C_{B3}, \ldots$are the shunt capacitances of capacitor banks

The cable capacitances are then introduced by the creation of dummy loops at the nodes where the shunt capacitances exist such that the total number of loops becomes $(n+m)$. The dummy loops are assigned loop numbers $n+1, n+2, \ldots n+m$. Extra rows and columns corresponding to the number of the created dummy loops are also added to each of the three network matrices to form partitioned matrices as shown,

$$R_{new} = \begin{bmatrix} R_{old} & A \\ A^T & Q \end{bmatrix} \quad (7)$$

$$L_{new} = \begin{bmatrix} L_{old} & B \\ B^T & H \end{bmatrix} \quad (8)$$

$$G_{new} = \begin{bmatrix} G_{old} & U \\ U^T & Z \end{bmatrix} \quad (9)$$

where U – is an $(n \times m)$ zero matrix, Q, H and Z are $(m \times m)$ diagonal matrices.

For a dummy loop, *p* created between two actual loops *i* and *j*:

$A_{ip} = A_{pi} = -R_{sp}$, $A_{jp} = A_{pj} = R_{sp}$, $Q_{pp} = R_{sp}$, elsewhere the entries are zero.

$B_{ip} = B_{pi} = -L_{sp}$, $B_{jp} = B_{pj} = L_{sp}$, $H_{pp} = L_{sp}$, elsewhere the entries are zero.

$U_{ip} = U_{pi} = 0$, $U_{jp} = U_{pj} = 0$, and $Z_{pp} = C_p^{-1}$, elsewhere the entries are zero.

where R_{sp} is the total resistance in the branch common to loops *i, j* and *p*;

L_{sp} is the total inductance in the branch common to loops *i, j* and *p*;

C_p^{-1} is the inverse of total shunt capacitance at *p*-th dummy loop.

Network Mesh Analysis

Mesh analysis was performed on the network to determine the instantaneous bus voltages, mesh currents using the partitioned matrices in (6) – (8) as the network model and voltage vectors to represent the sources and harmonic generating loads. It begins with simulation of non-linear loads to determine the instantaneous values of their distorted input current followed by the assembling of the voltage vector as the product of current vector and branch load impedance.

The required loop equation is,

$$L_{new}D^2I + R_{new}DI + G_{new}I = DV \quad (10)$$

where L_{new}, R_{new}, G_{new} are the updated loop inductance, resistance and inverse capacitance matrices respectively.

D – operator $\frac{d}{dt}$

I and *V* are the loop current and voltage vectors respectively.

$$D^2I = \begin{bmatrix} \frac{d^2i_1}{dt^2} \\ \frac{d^2i_2}{dt^2} \\ \vdots \\ \frac{d^2i_n}{dt^2} \end{bmatrix} \quad (11)$$

$$DI = \begin{bmatrix} \frac{di_1}{dt} \\ \frac{di_2}{dt} \\ \vdots \\ \frac{di_n}{dt} \end{bmatrix} \quad (12)$$

$$I = \begin{bmatrix} i_1 \\ i_2 \\ \vdots \\ i_n \end{bmatrix} \quad (13)$$

$$DV = \begin{bmatrix} \frac{dv_{s1}}{dt} \\ \frac{dv_{s2}}{dt} \\ \frac{dv_{s3}}{dt} \\ \vdots \\ \frac{dv_{sn}}{dt} \end{bmatrix} \quad (14)$$

Where vs_1, vs_2, vs_3, ... are the resultant applied voltages in the various network meshes

Determination of Distortion Profile

Overcurrent situation at each cable session is determined from the computed root mean square values, $\mathrm{I_{rms}}$, of current at each loop as well as their amplification factor. The distortion parameters of the loop currents are further computed in order to determine their complete distortion profile as a result of the presence of the non-linear loads. Firstly, the current vector is subjected to discrete Fourier Transform to obtain its harmonic spectrum which indicates the fundamental and harmonic components. The root-mean-square current is calculated thus;

$$I_{rms} = \sqrt{I_1^2 + \sum_{h=2}^{\infty} I_h^2} \quad (15)$$

$$I_{rms} = I_1 \sqrt{1 + \frac{\sum_{h=2}^{\infty} I_h^2}{I_1^2}} \quad (16)$$

where I_1 – represents the rms value of the fundamental current, I_h – the *h-th* harmonic component of current.

The total harmonic distortion (THD) is calculated thus,

$$THD = \frac{1}{I_1} \sqrt{\sum_{h=2}^{\infty} I_h^2} \quad (17)$$

Therefore, $$THD = \sqrt{\left(\frac{I_{rms}}{I_1}\right)^2 - 1} \quad (18)$$

Amplification Factor (AF) is defined in this study as ratio of the root mean square value of amplified loop current to the fundamental component,

$$I_{rms} = I_1 \sqrt{1 + THD^2} \quad (19)$$

$$AF = \frac{I_{rms}}{I_1} \quad (20)$$

Therefore, $$A_F = \frac{I_{rms}}{I_1} = \sqrt{1 + THD^2} \quad (21)$$

Journal of Engineering, Emerging Technologies and Applied Sciences
Volume: 03 Issue: 01 | March, 2026 Access point: https://www.ndu.edu.ng/jeetas

4. RESULTS AND DISCUSSION

The above methodology was applied to the given network in Figure 1 to determine suitable locations for the resonance mitigation devices. The computed network currents, THD values and Current Amplification were deployed for this purpose. The steady state values of loop currents, total harmonic distortion (THD) and overcurrent situation at the power line sections resulting from the mesh analysis on the given network are displayed in Tables 1 and 2. Considering only the induction furnaces as harmonic producing loads, the computed amplification factors in Table 1 are not significant enough to warrant any proposal for mitigation devise on the sample network.

Table 1: Amplification effect of Series Resonance on mesh currents of the sample network without Electric Arc Furnace

Meshes	Fundamental Current (A)	Total Current (A)	THD (%)	Amplification factor	% Increase
M1	3.68	4.33	61.94	1.1763	17.63
M2	12.85	13.02	16.30	1.0132	1.32
M3	60.79	60.83	3.89	1.0008	0.08
M4	117.70	117.73	2.36	1.0003	0.03
M5	166.65	166.68	1.81	1.0002	0.02
M6	45.16	45.24	5.83	1.0017	0.17
M7	104.55	104.57	2.19	1.0002	0.02
M8	178.22	178.23	1.20	1.0001	0.01
M9	34.84	34.90	6.07	1.0018	0.18
M10	4.85	5.20	38.33	1.0709	7.09

The case may be different if another network were to be used for the investigation or otherwise when the presence of an electric arc furnace (EAF) is considered (see Figure 3 and Table 2). The THD values and current amplification at different parts of the network are very high but notably in three particular locations which are in the neighbourhood of the three furnaces. Mesh analysis of network, without the filters in place, indicate that the percentage amplification of current are more pronounced at M1, M2, M6 and M10 sections of sample network with results 112 %, 55 %, 27 % and 298 % respectively. The pronounced influence of arc furnace on amplification levels presents the worst resonance scenario, and therefore forms the basis for deciding on the optimal location of the harmonic filter.

Table 2: Amplification effect of Series Resonance on mesh currents of the sample network considering the inclusion of Electric Arc Furnace

Meshes	Fundamental Current (A)	Total Current (A)	THD (%)	Amplification factor	% Increase
M1	3.68	7.78	186.31	2.1145	111.45
M2	12.83	19.83	117.81	1.5453	54.53
M3	60.69	64.45	35.73	1.0619	6.19
M4	118.80	123.32	27.83	1.0380	3.80
M5	167.31	68.99	14.24	1.0101	1.01
M6	43.93	55.56	77.46	1.2649	26.49
M7	106.15	112.07	33.87	1.0558	5.58
M8	179.88	182.29	16.42	1.0134	1.34
M9	34.80	39.17	51.65	1.1255	12.55
M10	4.85	19.30	385.58	3.9834	298.34

The current amplification at various meshes is also represented by the height of stems in Figures 2 and 3 which indicates that significant levels of current amplification occur at the M1, M2, M6 and M10 meshes near the locations of the furnaces. Hence, these sections of the network are more susceptible to resonance judging from these results, implying that the line conductors and equipment are under threat. They therefore constitute the high-risk areas and possible locations of the harmonic filters.

Journal of Engineering, Emerging Technologies and Applied Sciences
Volume: 03 Issue: 01 | March, 2026 Access point: https://www.ndu.edu.ng/jeetas

However, only one filter is proposed to mitigate the resonance situation in M1 and M2 sections, while separate filters need to be placed at M6 and M10 sections. The amplification effect of resonance is propagated to other network segments as shown.

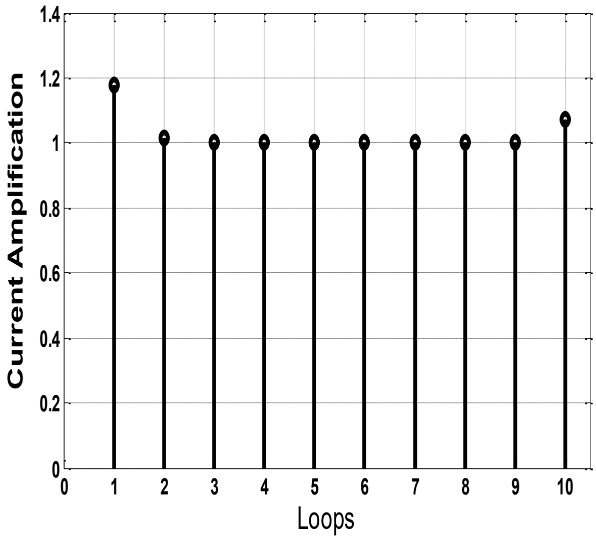

Figure 2: Overcurrent situation in all the loops of the given network neglecting the arc furnace

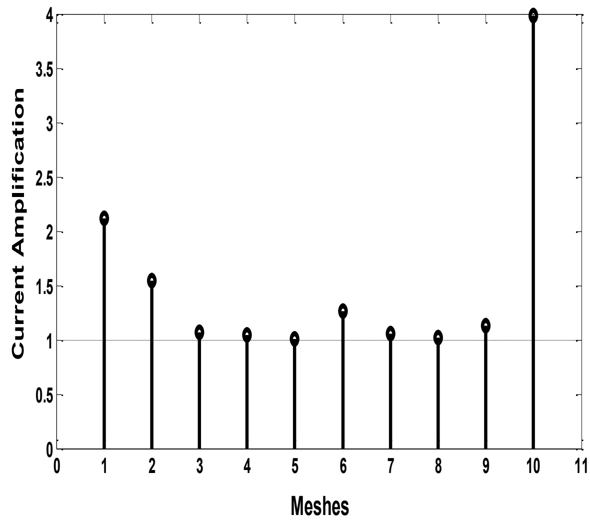

Figure 3: Overcurrent situation in all the loops of the given network while considering the inclusion of arc furnace.

Three passive filters were designed and connected at these three locations. The choice of filter parameters and ratings has been made according to the procedure presented in Kalunta *et al.* (2016). For the purpose of verifying the filter design, the mesh analysis was repeated in matlab environment with the filter connected to the network at the designated points to ascertain their impact on the network distortion profile, bus voltage and current amplification in the face of mitigation. The impedance of the filter branches are incorporated into the network by creating dummy loops at the connection points. The changes introduced by the application of the designed filters at the input sections of the furnaces in the first instance are shown in Figure 4 and 6, while the results of the second case are shown in Figures 5 and 7. The resulting magnitude of harmonic components of network currents at point of filter connection is shown in Figures 4 and 5. Connection of the designed filter branches at the designated locations of the sample network yielded a significant decrease in the peak magnitude of 5th harmonic current from 21.29% to 2.31% and almost an outright elimination of the 107th harmonic current. The result indicates significant reduction in the major harmonic frequencies implying that they constitute no more hazards to the network when the filters are applied. These curves indicate that some of the harmonic components are not totally eliminated, but the main harmonic components are drastically reduced and do not constitute a major contribution to the harmonic distortion. The mitigation of distortion by the application of filter branches in the case study at M1 is also analogous to a significant decrease in the total harmonic distortion (THD) from 186.31% to 3.12% in Table 3. This denotes a significant reduction in the harmonic magnitudes as well as firm validation of the proposed technique.

Journal of Engineering, Emerging Technologies and Applied Sciences
Volume: 03 Issue: 01 | March, 2026 Access point: https://www.ndu.edu.ng/jeetas

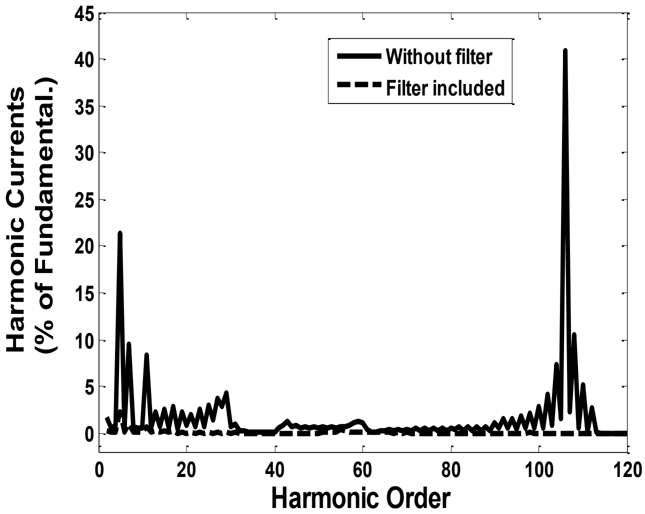

Figure 4: Reduction in harmonic content of mesh currents due to the injection of the proposed filter in the given network with only induction furnaces in place

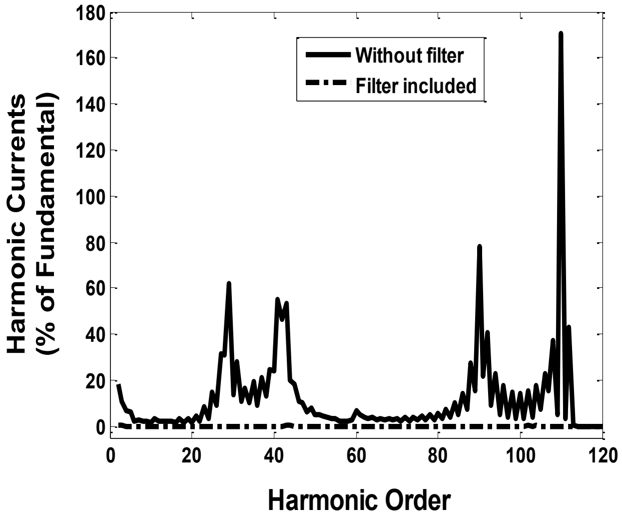

Figure 5: Reduction in harmonic content of mesh currents due to the injection of the proposed filter with both the induction furnace and arc furnace in place

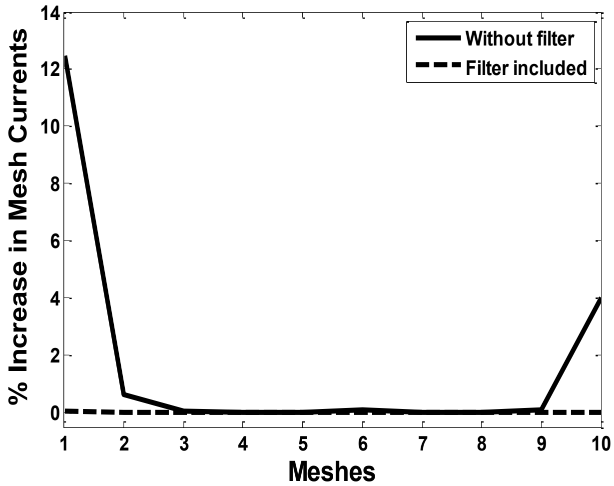

Figure 6: Changes in current amplification due to injection of filter in the network with only induction furnaces in place

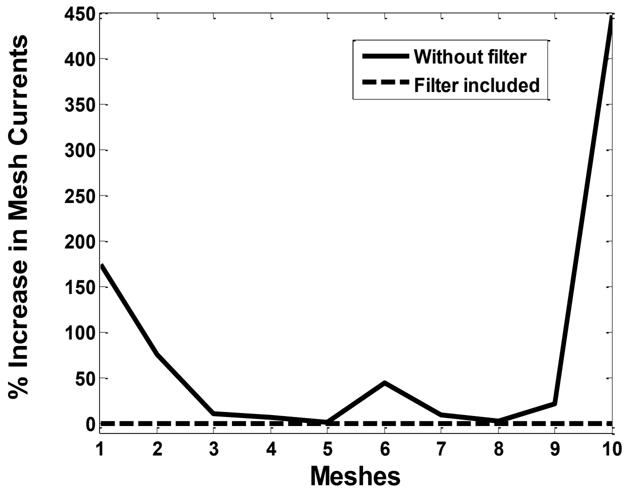

Figure 7: Changes in current amplification due to injection of filter in the given network and with the position of arc furnace considered

Table 3: Summary of analytical results from the application of the filter on the given network (with the arc furnace in place)

Meshes	Before Mitigation			After Mitigation		
	Mesh Current (Ampere)	Fundamental Current (Ampere)	THD (%)	Mesh Current (Ampere)	Fundamental Current (Ampere)	THD (%)
M1	7.78	3.68	186.31	2.20	2.20	3.12
M6	55.56	43.93	77.46	35.13	35.12	1.26
M10	19.30	4.85	385.58	12.83	12.81	6.34

4. CONCLUSION

The paper has identified the NITEL, NRC and Unilag buses as suitable locations of the proposed filters in the given network. The application of the designed filters in the series resonance mitigation has successfully reduced the distortion level and magnitudes of critical harmonic components as indicated by simulation of the network. Using the distortion profile of line currents as determinant for appropriate location of harmonic filters in electric distribution networks therefore proves to be a credible method. The process of using dummy loops to represent connection of cable capacitance has minimized the complexities involved in non-linear analysis of power networks thereby reducing the computer time. The proposed technique will assist Power Quality engineers in siting of harmonic filters for effective attenuation of resonant harmonic magnitudes at the design or modification stage of electric power networks. Appropriate location for the harmonic filters will successfully minimize the amplification of network currents in a series resonance scenario and also curb the associated economic losses.

REFERENCES

Abdel Aleem, S. H. E., Zobaa, A. F., Abdel Aziz, M. M. (2012). Optimal C-type passive filter based on minimization of the voltage harmonic distortion for non-linear loads. *IEEE Trans. Ind. Electronics*, **59**: 281–289.

Acha, E. and Madrigal, M. (2001). Power systems harmonics: Computer modelling and analysis. John Wiley and Sons Ltd., Chichester England, pp 52 – 53.

Bester, S. J. and Atkinson-Hope, G. (2012). Harmonic Filter Design to Mitigate Two Resonant Points in a Distribution Network, *Journal of Energy and Power Engineering* (6) 2018-2023.

Hooshman, R., Banejad, M. and Esfahani, M. (2008). A new time domain modelfor electric arc furnace. *Journal of Electrical Engineering*, **59** (4): 195 – 202.

Kalunta, F. O. and Okafor, F. N. (2015). Modeling of Rectifiers for Resonance Studies: A Pivotal Approach, *Proceedings of the Joint IEEE International Symposium on Electromagnetic Compatibility and EMC Europe*, Dresden Germany, August 16 – 22, 2015, pp 1380 -1387.

Kalunta F. O., Nnadi P. U., Akinbulire T. O. and Okafor F. N. (2016B). Design of harmonic filter for an electroplating plant. *Journal of Industrial Reasearch and Technology*, Federal Institute of Industrial Research Oshodi, Lagos, Nigeria, **5** (1): 71 – 81.

Kazeem, H. A., Albaloshi A. A., Al-Jabri A. S., and Al-Saidi K. H. (2005). Simple and advanced models for calculating single phase diode rectifier Line-side harmonics, *World Academy of Science, Engineering and Technology journal*, pp 179 – 183.

Liberado E. V., Souza W. A., Pomilio J. A., Paredes H. K. and Marafão F. P. (2013). Design of Static var Compensators using a General Reactive Energy Definition, *Przeglad Elektrotechniczny,* 89 (11) 233 – 238.

Manikandan P., Umayal S. P., Mariya A., Chithra M., and Ramachandran, M. (2013). Simulation and Hardware Analysis of Three Phase PWM Rectifier with Power Factor Correction, *IOSR Journal of Electrical and Electronics Engineering* (Volume 8) 27-33.

Md Hasan K.N., Rauma, K., Luna, A., Candela, J. I. and Rodriguez, P. (2012). Harmonic Resonance Study for Wind Power Plant**.** *International Conference on Renewable Energies and Power Quality (ICREPQ'12)*, Santiago de Compostela, Spain, 8th to 30th March 2012.

Mohammed F., Abdel Aleem H. E., Ibrahim A. M. and Zobaa A. F. (2014). Optimal sizing of C-type passive filters under non-sinusoidal conditions. *Journal of Energy Technology & Policy*, **1**(1): 35 – 44.

Pejovic, P. and Kolar, J. W. (2008). Exact Analysis of Three Phase Rectifiers with constant Voltage Loads, *IEEE Transaction on circuits and on circuits and systems II: Express Briefs*, Vol. 55 (8) 743 -747.

